Meshfree Simulation of Lung Deformation during Inspiration

S. Chhatkuli, H. Kojima, S. Koshizuka., and M. Uesaka

***Abstract*— A meshfree simulation technique called Moving Particle Semi-implicit method (MPS) is applied to simulate deformation of lung and a tumor inside the left lung during inspiration. Deformation is modeled by considering the lung tissues to be homogenous, isotropic and viscoelastic. The regional deformation of lung and a tumor in a Superior-Inferior (SI), Right-Left (RL) and Anterior-Posterior (AP) direction is compared with the experimental CT data taken at the end of inspiration. The deformation predicted by numerical simulation matches reasonably well with the experimental results.**

***Index Terms*—CT, MPS, Numerical Modeling.**

I. Introduction

Soft biological tissues are highly viscoelastic in nature and, in particular, lung tissues have been recognized to be viscoelastic as early as 1939 [1]. Lung tissues, which are highly deformable soft biological tissues, exhibit large deformation during breathing. While breathing, tumor inside the lung will also undergo displacement or deformation. However, among other factors, the extent of deformation/displacement depends largely on its location in the lung. Hence, the information on lung deformation during breathing is particularly very crucial in radiation treatment planning for lung tumor.

There are some experimental works performed to understand the deformation of lung during breathing or during change in body position.

Mori *et. al*. did study on lung tumor displacement by using four dimensional Computed Tomography (CT) techniques on 14 patients. They noticed that the total displacement in the lower lobe was around twice the middle or upper lobe [2].

[3] performed posture dependent human lung imaging in an open access MRI system. The study showed that when the lungs were oriented in upright position from supine position, the lungs were distended modestly.

Considering the numerical modeling of lung deformation during breathing, majority of such works has been done by applying finite element technique. Nakao *et. al.* treated lung as an elastic object and analyzed the deformation based on linear finite element method [4]. Didier *et. al.* considered lung tissue as homogeneous, isotropic and its constitutive equation defined by a linear elastic behavior and simulated lung deformation by using finite element method [5]. Villard *et. al.* used finite element method to simulate lung deformation during breathing and measured the influence and relevance of mechanical parameters [6]. They suggested that Young modulus can be chosen arbitrarily; However, Poisson's ratio plays a significant role and may not be chosen arbitrarily for correct prediction. In several literatures, Poisson's ratio ranging from 0.25 to 0.47 has been chosen to model lung deformation during breathing [7].

Since soft biological tissues, like lung, exhibit the property of high deformation under application of external pressure, grid based technique like finite element method might suffer from grid distortion at some point. Hence, a gridless method called Moving Particle Semi-implicit (MPS) method is proposed in this paper as an alternative method to simulating lung deformation during breathing considering it to be homogenous, isotropic and viscoelastic. In gridless technique like MPS, grid generation is not necessary. The elastic solids are represented by a collection of finite number of particles. During the simulation, the changes in physical properties of particles while they undergo displacements are calculated.

The MPS method has been first introduced by Koshizuka and Oka [8] in 1996 for fluid dynamics. In 2001, Chikazawa *et. al.* [9] presented the particle method for elastic and visco-plastic structures and fluid–structure interaction. In their study, particle method was proposed for thick elastic and visco plastic structures based on the concept of MPS method which provided particle interaction model for differential operators. [10], [11] applied MPS method for dynamic simulation of elastic solids. They did the numerical modeling of elastic behavior, large deformation and fracture of elastic solid of different materials. Three dimensional elastic analysis and large deformation of soft material was performed by [12].

II. GOVERNING EQUATIONS

As in fluid mechanics, the governing equation of motion of a viscoelastic solid can be written as (1) [8], [9] and [13].

$$\rho \frac{d\mathbf{v}}{dt} = \frac{\partial}{\partial x}\left(-P + \sigma^{\alpha\beta}\right) + \kappa\nabla^2\mathbf{v} + \rho K_{ext} \qquad (1)$$

Here,

Manuscript received May 20, 2009.

S. Chhatkuli is with the University of Tokyo, Department of Nuclear Engineering and Management, 2-11-6 Yayoi, Bunkyo-ku, Tokyo, Japan (+81—3-5841-2916; e-mail: subas@nuclear.jp)

H. Kojima is with the University of Tokyo, Department of Nuclear Engineering and Management, 2-11-6 Yayoi, Bunkyo-ku, Tokyo, Japan (e-mail: hkojima@nuclear.jp)

S. Koshizuka is with the University of Tokyo, Department of Quantum Engineering and System Science, 7-3-1, Hongo, Bunkyo-Ku, Tokyo 113-8656, Japan (e-mail: koshizuka@q.t.u-tokyo.ac.jp)

M. Uesaka is the University of Tokyo, Department of Nuclear Engineering and Management, 2-11-6 Yayoi, Bunkyo-ku, Tokyo, Japan (e-mail: uesaka@nuclear.jp)

$$P = -\lambda \varepsilon^{\gamma\gamma} \quad (2)$$

$$\sigma^{\alpha\beta} = 2\mu\varepsilon^{\alpha\beta} \quad (3)$$

$$\lambda = \frac{E\nu}{(1+\nu)(1-2\nu)} \quad (4)$$

$$\mu = \frac{E}{2(1+\nu)} \quad (5)$$

where, ρ is density of material, P an isotropic pressure which is obtained in particle location , $\sigma^{\alpha\beta}$ unisotropic components of stress tensor which is obtained between the particles, λ and μ the Lame constant, κ the viscosity, K_{ext} external force acting on the particles, E Young modulus and ν Poisson's ratio.

III. NUMERICAL MODEL

A. Particle Interaction Model

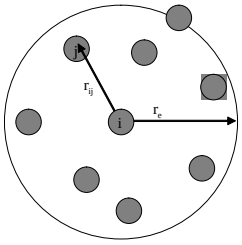

Fig. 1 Particle interaction model

In MPS method, as shown in Fig. 1, viscoelastic solid is represented as a collection of finite number of particles. Particles behave as if they are connected by normal and shear springs which are governed by the parallel (normal) and perpendicular (shear) displacement of the particles.

As show in Fig. 1, particles interact with its neighboring particles covered with a weight function as (6).

$$w(r_{ij}) = \begin{cases} \frac{r_e}{r_{ij}} - 1 & (r_{ij} \le r_e) \\ 0 & (r_{ij} > r_e) \end{cases} \quad (6)$$

The global accuracy in particle methods depends on the initial distribution of particles. It is recommended that a finer particle distribution model and approximately large particle number be used according to the available computer resources to obtain better computational results [14], [15].

B. Calculation of Isotropic Pressure

Isotropic pressure (2) is represented as divergence of strain in the particle method [9]. Divergence in particle method is represented as (7).

$$\varepsilon^{\gamma\gamma} = \mathrm{div}(\vec{u}_{ij}) = \sum_{j \ne i} \frac{d}{n_0} \cdot \frac{\vec{u}_{ij} \cdot \vec{r}_{ij}^{\,o}}{\left|\vec{r}_{ij}^{\,o}\right|^2} w\left(\left|\vec{r}_{ij}^{\,o}\right|\right) \quad (7)$$

where, d is the number of spatial dimension, $\vec{u}_{ij}$ the displacement vector, $\vec{r}_{ij}^{\,o}$ the initial position vector, $w\left(\left|\vec{r}_{ij}^{\,o}\right|\right)$ the initial weight function and n_0 the initial particle number density. Particle number density at coordinate $\vec{r}_i$ where particle i is located is defined as

$$< n_0 > i = \sum_{j \ne i} w\left(\left|\vec{r}_j - \vec{r}_i\right|\right) \quad (8)$$

C. Calculation of Unisotropic Stress

Unisotropic stress (3) is calculated by using (9).

$$\sigma^{\alpha\beta} = 2\mu\varepsilon^{\alpha\beta} = 2\mu \frac{(\vec{u}_{ij})}{\left|\vec{r}_{ij}^{\,o}\right|} \quad (9).$$

D. Calculation of Laplacian

The diffusion term in (1) is calculated by using the Laplacian model [13] as in (10)

$$\left\langle \nabla^2 \Phi \right\rangle_i = \frac{2d}{n_0} \sum_{j \ne i} \frac{\Phi_j - \Phi_i}{\left|\vec{r}_{ij}^{\,o}\right|^2} w\left(\left|\vec{r}_{ij}^{\,o}\right|\right) \quad (10)$$

E. Calculation of Divergence Terms

The divergence terms in (1) are calculated as (11) and (12) respectively.

$$\frac{\partial P}{\partial x^\alpha} = \sum_{j \ne i} \frac{d}{n_0} \frac{P_i \vec{r}_{ij}}{\left|\vec{r}_{ij}^{\,o}\right|^2} w\left(\left|\vec{r}_{ij}^{\,o}\right|\right) \quad (11)$$

$$\frac{\partial \sigma^{\alpha\beta}}{\partial x^\beta} = \sum_{j \ne i} \frac{d}{n_0} \frac{\sigma^{\alpha\beta}}{\left|\vec{r}_{ij}^{\,o}\right|} w\left(\left|\vec{r}_{ij}^{\,o}\right|\right) \quad (12)$$

The velocity and the corresponding coordinates at a new time step is then updated by using a fourth order Runge Kutta scheme.

Time step is selected in the computation to satisfy the following Courant condition:

$$\Delta t \le 0.2 \frac{\Delta l}{U_{max}} \quad (13)$$

where Δl is the original distance between two particles and U_{max} the maximum velocity among all particles.

Rotation of particle is calculated by updating the angular velocity and rotation angle [10].

IV. VALIDATION TEST

An ability of the model to simulate the deformation of lung during breathing was performed beforehand. Dynamic tracking of lung deformation during inspiration was performed for the lower and upper lobe of a lung. The numerical results have been compared against the experimental results obtained by tracking the movement of a gold marker placed at those locations.

Mean squared error between numerical results and experimental results were obtained as 2 mm (Fig. 2) for the lower lobe and 1 mm (Fig. 3) for the upper lobe.

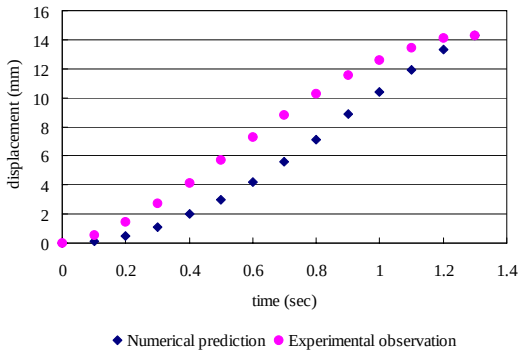

Fig. 2 Displacement of lower lobe during inspiration

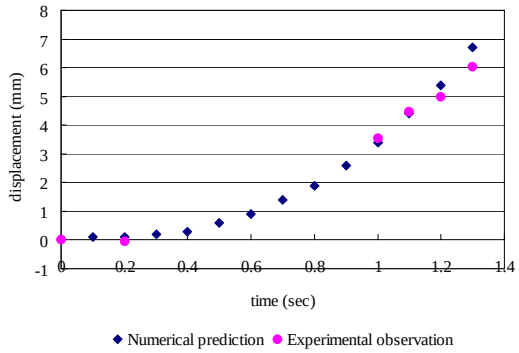

Fig. 3 Displacement of upper lobe during inspiration

V. NUMERICAL EXPERIMENT

To simulate the lung distension during inspiration, a 3D model of a right and a left lung attached to a trachea was generated from 70 slices of CT data taken at the beginning of inspiration. A tumor with a prominent shape and size was located in the left lung.

In the numerical simulation, the 3D model was converted to particle model by considering each voxel of the 3D model as a particle. The particle model was created from 21296 uniformly distributed particles with a spacing of 5 mm.

During inspiration, diaphragm moves downward and the rib cage moves forward. Hence, a negative pressure develops around the external surface of the lung. To compensate for that pressure, air flow inside the lungs into alveoli through trachea and, hence, causes volumetric expansion of lung. Along the Anterior-Posterior (AP) direction and Right-Left (RL) direction lung displacement is limited due to the presence of rib cage. However, in the Superior-Inferior direction (SI) lung has much mobility as in normal inspiration condition diaphragm moves down by 3-4 cm.

To simulate the behavior of lung expansion, radial outward pressure was applied at the bottom lung particles. In the numerical experiment, Poisson's ratio (ν) was selected as 0.46, Young Modulus (E) as 780 pa, viscosity (κ) as 0.013 m^2/s and density as 960 kg/m^3 as the mechanical property of the lung and tumor tissues.

The computation was done in Intel® Core™2 Duo Processor and the computation time was about 3 hours.

A. Results and Discussion

The simulated results of the lungs and a tumor deformation in AP, RL and SI direction, during inspiration, are compared with the CT data taken at the beginning and the end of inspiration.

Fig. 4 shows the initial and deformed shape of lung obtained from experimental results and numerical simulation. The experimental results shows that the deformation at the lower portion of the lungs is much prominent compared to the upper portion. Fig. 4 shows that the deformed shape was realistically simulated by the numerical model.

Fig. 5 shows the schematic view of the expanded lung. In the figure, expansion obtained in SI, AL and AP direction from the CT images and numerical results is compared. The expansion value inside the parenthesis in Fig. 5 represents the simulated value.

The experimental results showed that the total expansion of right lung along SI direction was 25 mm (Fig. 5). The numerical simulation showed that the elongation of right lung along SI direction was 23 mm. Likewise, for the left lung, the experimental results showed that the total expansion along SI direction was also 25 mm. The numerical model predicted the expansion accurately for the left lung (Fig. 5).

Considering an enlargement of lung in RL direction, the experimental results showed the expansion at upper part for right lung and left lung was 1 mm and 4 mm respectively (Fig. 5). However, the numerical model predicted no expansion at those locations.

At the lower part, the expansion in RL direction for right and left lung was 2 mm and 1 mm respectively. At that position, the numerical simulation predicted the expansion for right lung and left lung was 5 mm and 1 mm respectively.

The experimental results showed that along the AP direction, in the lower part (Fig. 5), enlargement of right and left lung was 3 mm and 5 mm respectively. The numerical results showed that the enlargement along AP direction for right and left lungs was 4 mm and 5 mm respectively.

Considering the tumor, both the experimental and numerical prediction shows that there was no volumetric change in tumor shape (Fig. 6) by the end of inspiration. The volume of tumor was about 60 cm^3 at the beginning and end of inspiration. However, the experimental and numerical results showed that the center point of the tumor position was lowered by less than 5 mm at the end of inspiration, along SI direction. The comparatively lower displacement of tumor might be partly due to its location in the lung.

Fig. 7 shows the simulated result of overall deformation, along SI direction, at the lung surface by the end of inspiration. The results showed that the deformation varies from less than 5 mm in upper part to over 20 mm in the lower part.

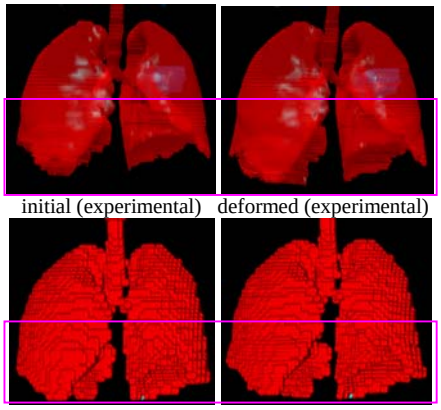

Fig. 4 Lung at the beginning and end of inspiration

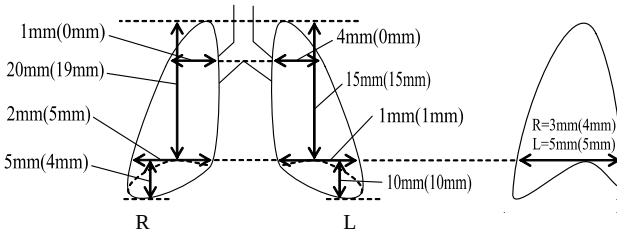

Fig. 5: Schematic view showing the total expansion of the lungs in SI, RL and AP direction. The value in the parenthesis represents the simulated expansion.

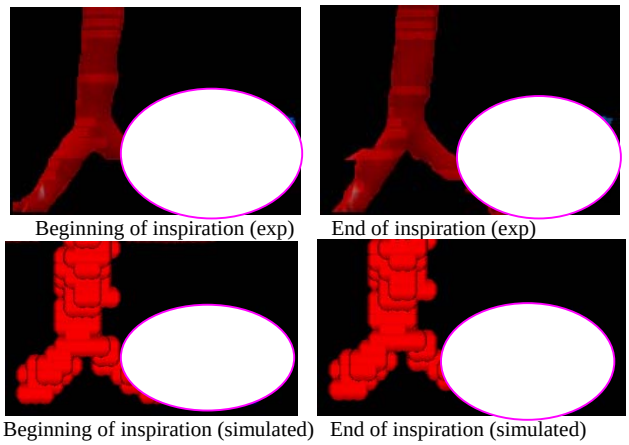

Fig. 6 Tumor at the beginning and end of inspiration

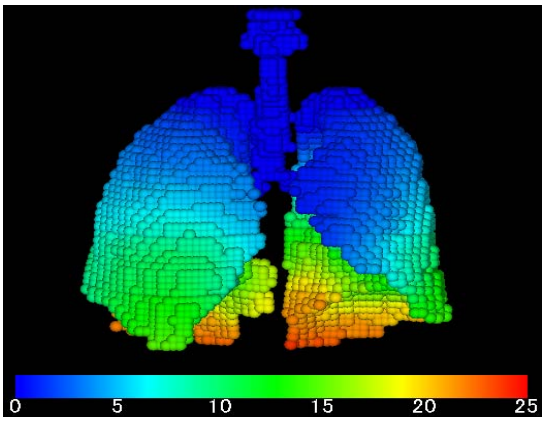

Fig.7 Simulated result of lung deformation (mm) along SI direction during inspiration

VI. CONCLUSION

A meshfree simulation of the lungs and a tumor deformation during inspiration is presented considering the lung tissues to be homogeneous, isotropic and viscoelastic.

Comparing the numerical results with the experimental results, the deformation of the lungs in SI, RL and AP direction during inspiration was simulated realistically with reasonable accuracy. The variation of lung deformation from the upper to the lower lobe was predicted realistically. Moreover, displacement of a tumor inside the left lung was also well simulated by this technique.An ability of the model to simulate the deformation of lung during breathing was performed beforehand. Dynamic tracking of lung deformation during inspiration was performed for the lower and upper lobe of a lung. The numerical results have been compared against the experimental results obtained by tracking the movement of a gold marker placed at those locations. Mean squared error between numerical results and experimental results were obtained as 2 mm (Fig. 2) for the lower lobe and 1 mm (Fig. 3) for the upper lobe.

REFERENCES

[1] L. E. Bayliss, and G. W. Robertson, “The visco-elastic properties of the lungs” *Q. J. Exp. Physiol*., vol. 29, pp. 27-47, 1939.

[2] S. Mori, M. Endo, S. Komatsu, T. Yasahiro, S. Kandatsu, and M. Baba, “Four dimensional measurement of lung tumor displacement using 256 multi slice CT scanner” *Lung Cancer*., vol. 56, pp. 59-67, 2007.

[3] L. L.Tsai, R. W. Mair, C. Li, M. S. Rosen, S. Patz, and R. L. Walsworth, “Posture-dependent Human 3He Lung Imaging in an Open-access MRI System1: Initial Results” *Academic radiology*., doi.org/10.1016/j.acra.2007.10.010

[4] M. Nakao, A. Kawashima, M. Kokubo, and K. Minato, “Simulating lung tumor motion for dynamic tumor tracking irradiation” *IEEE Nuclear Sciences Symposium Conference Record*., pp 4549-551, 2007.

[5] A. Didier, P. Villard, J. Bayle, M. Beuveand, and B. Shariat, “Breathing thorax simulation based on pleura physiology and ribe kinematics” *IEEE Medical Information Visualisation- BioMedical Visualisation*., 2007.

[6] P. Villard, M. Beuve, B. Shariat, V. Baudet, and F. Jaillet, “Simulation of lung behaviour with finite elements: Influence of bio mechanical parameters” *Proceedings of the Third International Conference on Medical Information Visualisation- Biomedical Visualisation*., 2005.

[7] A. Al-Mayah, J. Moseley and K. K. Brock, “Contact surface and material nonlinearity modeling of human lungs” *Physics in Medicine and Biology*, doi:10.1088/0031-9155/53/1/022

[8] S. Koshizuka, and Y. Oka, “Moving-particle semi-implicit method for fragmentation of incompressible fluid” *Nuclear Science and Engineering*., vol. 123, pp 421-434, 1996.

[9] Y. Chikazawa, S. Koshizuka, and Y. Oka, “A particle method for elastic and visco-plastic structures and fluid-structure interactions” *Computational Mechanics*., vol. 27, pp 97-106, 2001.

[10] M. Song, S. Koshizuka, and Y. Oka, “A particle method for dynamic simulation of elastic solids” *proc. WCCM VI in conjunction with APCOM*., Beijing, 2004.

[11] M. Song, S. Koshizuka, and Y. Oka, “Moving particle semi-implicit (MPS) method for solid simulation”. *proc. of ICAPP*., Seoul, 2005.

[12] S. Koshizuka, M. Song, and Y. Oka, “A particle method for three-dimensional elastic analysis” *proc. WCCM VI in conjunction with APCOM*., Beijing, 2004.

[13] S. Zhang, K. Morita, K. Fukuda, and N. Shirakawa, “An improved MPS method for numerical simulations of convective heat transfer problems” *Int. J. Numer. Meth. Fluids*., vol. 15, pp. 31-47, 2006.

[14] J. Monaghan, H. E.Huppert, and M. G.Worster, “Solidification using smooth particle hydrodynamics” *Journal of Computational Physics*., vol. 206, pp 684-705, 2005.

[15] R. Speith, and H. Riert, “The viscous gas ring as an astrophysical test problem for a viscous SPH code” *Journal of Computational and Applied Mathematics*., vol. 109, pp 231-242, 1999.